

SIMULATION ON BUILDUP OF ELECTRON CLOUD IN RAPID CYCLING SYNCHROTRON OF CHINA SPALLATION NEUTRON SOURCE *

Liu Yu-Dong[#], Li Kai-Wei, Wang Sheng, Huang Liang-Sheng
IHEP, CAS, Beijing 100049, China

Abstract

Electron cloud interaction with high energy positive beam are believed responsible for various undesirable effects such as vacuum degradation, collective beam instability and even beam loss in high power proton circular accelerator. An important uncertainty in predicting electron cloud instability lies in the detail processes on the generation and accumulation of the electron cloud. The simulation on the build-up of electron cloud is necessary to further studies on beam instability caused by electron cloud. China Spallation Neutron Source (CSNS) is the largest scientific project in building, whose accelerator complex includes two main parts: an H- linac and a rapid cycling synchrotron (RCS). The RCS accumulates the 80MeV proton beam and accelerates it to 1.6GeV with a repetition rate 25Hz. During the beam injection with lower energy, the emerging electron cloud may cause a serious instability and beam loss on the vacuum pipe. A simulation code has been developed to simulate the build-up, distribution and density of electron cloud in CSNS/RCS.

INTRODUCTION

In high intensity proton circular accelerator, the electron cloud effect has been considered as one of the main sources of beam instability, which can lead to the uncontrolled beam loss [1]. This electron proton instability has been observed and confirmed in many commission proton circular accelerators, such as LANL PSR [2], KEK Booster [3], CERN PS [4] and SNS in ORNL [5]. The primary electrons produced by proton losses at the chamber surface attracted and accelerated by the body of bunch then released at the bunch tail or bunch spacing. The secondary electrons are produced and amplified when the accelerated electron hitting the chamber wall. This secondary electron multipacting attributes to the main source of electron cloud.

Table 1: The main parameters of the RCS/CSNS

Parameters	Injection	Extraction
Circumference C (m)	227.92	227.92
Energy E (GeV)	0.08	1.6
Bunch Population N_p (10^{13})	1.56	1.56
Revolution Frequency ω (MHz)	3.20	6.78
Bunch length σ_p (m)	48.931	22.285
Beam transverse size σ_x, σ_y (cm)	1.5, 1.5	1.2, 1.2
Pipe radius b (cm)	10	10

*Work supported by National Natural Science Foundation of China (11275221, 11175193)
[#]liuyd@mail.ihep.ac.cn

A high intensity proton accelerator facility as neutron source proposed in past ten years and is being built in China, which is named China Spallation Neutron Source (CSNS) [5]. The facility is equipped with an H- linac and a rapid cycling synchrotron (RCS). A simulation code has been developed and benchmarked to ascertain detailed establishment of electron cloud in CSNS/RCS. The physical mechanism on primary electron production, its dynamics, secondary electron emission and electron accumulation is described in section II of this paper. By tracking dynamics of electrons with physical model in section II, a simulation code for obtaining distribution and density of electron cloud has been developed and benchmarked with other machines. With the beam parameters of RCS/CSNS, the process of electron cloud buildup is studied in different simulation conditions such as average beam loss rate, secondary electron yield, transverse and longitudinal beam profile, and beam intensity. Most of the simulations are performed in a field-free region mainly. The comprehensive simulation on electron cloud in RCS/CSNS gives the quantitative relation between electron density and beam parameters which is meaningful to the construction of RCS/CSNS.

PHYSICAL MODEL

The electron sources in proton circular accelerator may be classified into (1) electrons stripped at injection region; (2) electrons produced by proton loss incident the vacuum chamber; (3) secondary electron emission process; and (4) electrons produced by residual gas ionization. The stripped electrons generated near the stripping foil, which can be absorbed by installing a special collector at the injection region [7]. The yield of ionization electrons is determined by the ionization cross section and vacuum pressure in beam chamber. Because of the lower vacuum pressure about 10^{-7} Pa and ionization cross section for CO and H₂ approximately 1.3 MBar and 0.3 MBar, the ionization electrons can be neglected in simulation. In the electron dynamic tracking for RCS/CSNS, the primary electrons produced by proton losses and secondary electrons are considered.

These striking electrons may produce secondary electrons if their energy is high enough. The fraction between the emission electrons from pipe surface and the total incident electrons is defined as secondary electrons yield (SEY). If SEY is above 1, the electrons multipacting will happen. Actually, the secondary electrons include two types: elastic backscattered electrons and true secondary electrons. The yields of the true secondary electrons and elastic backscattered electrons can be expressed with formula (1) and (2) [8], respectively. In formula, δ_{max} is the

Content from this work may be used under the terms of the CC BY 3.0 licence (© 2015). Any distribution of this work must maintain attribution to the author(s), title of the work, publisher, and DOI.

maximum secondary emission yield for perpendicular incidence, and ε_{max} presents the incidence electron energy with maximum secondary emission yield δ_{max} . E_p is the energy of the electron, θ the angle of incidence electrons and $\hat{\delta}_e, \delta_{e,\infty}, \Delta$ and E_e are experimental fitting parameters decided by pipe material with $\hat{\delta}_e = 0.1$, $\delta_{e,\infty} = 0.02$ and $\Delta = E_e = 5eV$ [8].

$$\delta_{se}(E_p, \theta) = \delta_{max} \times \frac{1.44 \times (E_p / \varepsilon_{max})}{0.44 + (E_p / \varepsilon_{max})^{1.44}} \exp(0.5 \times (1 - \cos(\theta))) \quad (1)$$

$$\delta_e(E_p) = \delta_{e,\infty} + \hat{\delta}_e - \delta_{e,\infty} \exp\left(\frac{-(E_p - E_e)^2}{2\Delta^2}\right) \quad (2)$$

In the magnetic-field-free region, the electrons move under the space-charge fields of the proton beam and between other electrons. For the long proton bunch, the longitudinal space-charge field can be neglected due to slow potential variations in longitudinal direction and the symmetry of longitudinal beam profile that traps the particles longitudinally. Therefore, the electrons mainly move under the beam transverse fields. For a cylindrical beam with uniform and gaussian transverse distribution, the space-charge fields are expressed respectively as

$$E_r(t) = \begin{cases} \frac{\lambda(t)}{4\pi\varepsilon_0} \frac{2}{r} & (r > \sigma_r), \\ \frac{\lambda(t)}{4\pi\varepsilon_0} \frac{2r}{\sigma_r^2} & (r < \sigma_r), \end{cases} \quad (3)$$

$$E_r(t) = \frac{\lambda(t)}{4\pi\varepsilon_0} \left[1 - \exp\left(-\frac{r^2}{2\sigma_r^2}\right)\right] \frac{2}{r} \quad (4)$$

where $\lambda(t)$ is the beam's line density, ε_0 known as the permittivity of vacuum, and σ_r is the beam transverse size. In fact, the space-charge fields of any spatial particle distribution can be obtained by numerical evaluation with PIC methods, which meshes the particles in three dimensional grid and makes two dimensional FFT in the transverse grids for each longitudinal slice to compute the potential on every grid point. The electric field comparison between numerical solution and analytical solution to uniform and Gaussian distributed charge are shown in figure1. It is clear the numerical solution fits well to the analytical results.

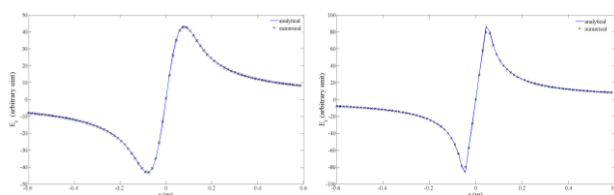


Figure 1. Electric field with different particle distribution (left: uniform; right: Gaussian)

During the passage of proton bunch, the electrons feel the beam action and make a nearly periodic oscillation with a slow time dependence given by the beam line density $\lambda(t)$. Assuming the bunch is uniform in the longitudinal direction with bunch population 1.56×10^{13} in CSNS/RCS, the oscillation frequency ranges from 20.23 MHz to 134.84 MHz. In the simulation model, electron cloud formation is estimated by tracking the motion of electrons produced by

primary and secondary electron emission. The vacuum chamber is assumed to be a cylindrical perfect conducting pipe. The primary electrons generated by lost protons hitting vacuum chamber wall is $Y * P_{loss}$ per turn for whole ring, where Y is effective electron yield per lost proton, and P_{loss} is proton loss rate per turn for the whole ring per beam proton. The lost proton distribution is proportional to the instantaneous bunch intensity. The electrons are represented by macroparticles. The secondary electron mechanism adds to a variable number of macroparticles, generated according to SEY model mentioned before. The proton bunch is sliced into equal-size steps longitudinally and each slice has a local proton density $\lambda(t_i)$. Electrons are tracked step by step along the passage of proton beam. The equation of motion for electrons is expressed by

$$\frac{d^2x(t)}{dt^2} = -2\lambda_p(t_i) r_e c^2 F_G[x(t)] \quad (5)$$

Where r_e is the classical electron radius, F_G is the normalized electric force determined by equation (3) and (4). For proton bunch in CSNS/RCS, the longitudinal profile is sinusoidal function expressed as

$$\lambda_p(t_i) = \frac{\pi N_p}{2\sigma_p} \sin\left(\frac{\pi v t_i}{\sigma_p}\right) \quad (6)$$

Where σ_p is the longitudinal length of proton bunch and v is bunch velocity.

SIMULATION RESULTS

According to the physical model described in section II, a simulation code was developed independently to understand the buildup of electron cloud in proton circular accelerator. After verifying the validity of simulation by benchmarking electron cloud density in J-PARC, LANL PSR and ORNL SNS, the buildup of the electron cloud in CSNS/RCS is simulated in different parameters, such as proton loss rate, SEY, beam intensity and bunch transverse size. For high intensity proton accelerator, the common requirement of loss power for maintenance is lower than 1 W/m. assuming the beam loss happen in first several hundred turns and every lost proton can produce 100 electrons [9], the densities of electron cloud in series of P_{loss} are shown in figure 2.

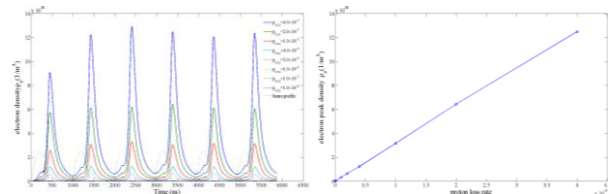


Figure 2. The densities of electron cloud in different proton loss rate

It is clear that the peak density of electron cloud linearizes to the proton loss rate because of the thinner density of electron cloud whose line density λ_e is only about 2% proton average line density λ_p . The transverse distribution of electrons in the vacuum pipe with the passage of proton bunch for CSNS/RCS 80 MeV during the injection is shown in figure 3.

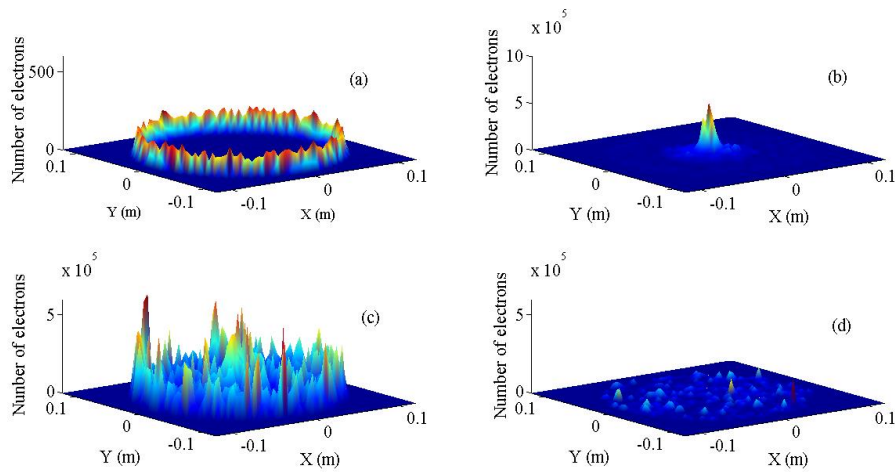


Figure 3. Transverse distribution of electron cloud during a bunch passage.
 (a: bunch head; b: bunch center; c: bunch tail; d: bunch gap)

It is clear the electrons are produced near the pipe wall and distributed widely at the start of interaction with the bunch. Then electrons are gathered to the beam vicinity and cloud size is comparable to beam size. After the bunch passage and without interaction, these accumulated electrons splash in the vacuum pipe. During the passage of the next bunch, the same process will happen again.

The electron cloud amplification in various δ_{max} is simulated for CSNS/RCS and the results are shown in figure 4. It is clear that the peak electron cloud density is sensitive to the maximum secondary electron yield. So the most efficient method to cure the electron cloud is surface treatment to reduce δ_{max} below 1.3.

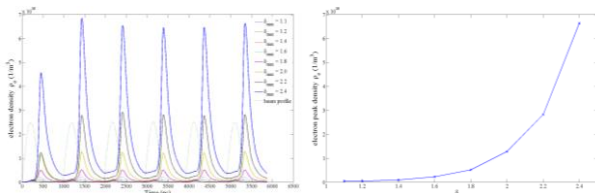


Figure 4. The electron cloud with various δ_{max}

The energy of primary electrons is decided by the loss protons. In order to understand the relation between primary electron characteristics and electron cloud, the development of electron cloud in different primary electrons energy is simulated and shown in figure 5.

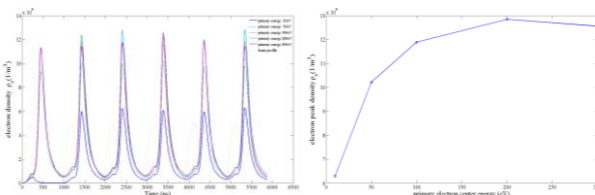


Figure 5. Electron cloud vs primary electron energy

The beam transverse size also has much influence on the saturation density of the electron cloud because of the beam space-charge fields expressed in equation (3) and (4). The simulation on electron cloud under different beam transverse size is shown in figure 6. Broadening the beam

size gradually, electron energy gain drops lower to the ϵ_{max} and the cloud density descends correspondingly.

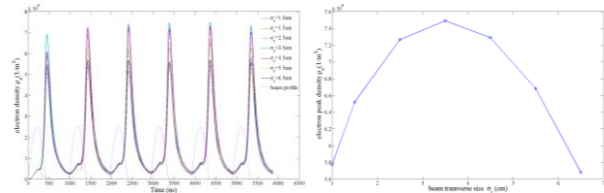


Figure 6. Electron cloud density vs beam transverse size

The electron cloud buildup in different beam intensity is plotted in figure 7. With stronger beam intensity, primary electrons produced by beam loss increase correspondingly and their energy gain is enhanced simultaneously.

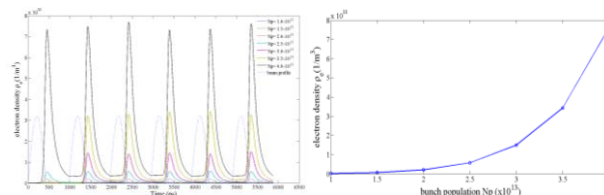


Figure 7. Electron cloud density vs beam intensity

CONCLUSION

For instance of CSNS/RCS, the buildup of electron cloud in circular proton accelerator was investigated. A computer simulation code is developed to study the accumulation process of electron cloud. In the simulation model, primary electrons appear due to proton loss on the wall of vacuum pipe and the secondary electron emission model is also included. The calculation proved the application on TiN coating to reduce the secondary yield is a powerful cure for electron cloud. The investigation on the electron cloud buildup in various beam parameters such as beam intensity, transverse size and proton loss rate, is done in detail. All these simulation will be meaningful to understand the interaction between electrons and high intensity proton beam in circular accelerators.

REFERENCES

- [1] D. Neuffer, E. Colton, et al. "Observations of a fast transverse instability in the PSR" Nucl. Instrum. Methods Phys. Res., Sect. A 321, 1(1992).
- [2] R. Macek, "Overview of the Program Plan and the Experimental Results from PSR", LBLN Workshop on the e-p instability, November, 20-21, 2000.
- [3] Y. Irie, et al, "Observation and Modeling of Electron Cloud Instability", KEK Proc. 97-17, (1997) pp 247-255.
- [4] R. Cappi, G. Metral, could be found at website: <http://www.cern.ch/PSdoc/ppc/md/md980716/epinstab.html>.
- [5] V. V. Danilov et al., Accumulation of High Intensity Beam and First Observations of Instabilities in the SNS Accumulator Ring, HB2006, p.59.
- [6] Wang S, Fang S X, Fu S N et al., "Introduction to the overall physics design of CSNS accelerators", Chin. Phys. C, 2009, 33(S2): 1-3.
- [7] L. F. Wang, D. Raparia, J. Wei, and S.Y. Zhang, "Mechanism of electron cloud clearing in the accumulator ring of the Spallation Neutron Source", Phys. Rev. ST Accel. Beams, Volume 7, 034401 (2004).
- [8] M.A. Furman and G. R. Lambertson, "The Electron Cloud Effect in the arcs of the PEP-II Positron Ring", KEK Proceedings 97-17, p. 170 (1997).
- [9] P. Thieberger et al, "Secondary-electron yields and their dependence on the angle of incidence on stainless-steel surfaces for three energetic ion beams", Phys. Rev. A 61, 042901 (2000).